energies

MDPI

Article

Hybrid Surrogate Model-Based Multi-Objective Lightweight Optimization of Spherical Fuel Element Canister

Yuchen Hao, Jinhua Wang, Musen Lin, Menghang Gong, Wei Zhang, Bin Wu, Tao Ma, Haitao Wang, Bing Liu and Yue Li *

Key Laboratory of Advanced Reactor Engineering and Safety of Ministry of Education, Collaborative Innovation Center of Advanced Nuclear Energy Technology, Institute of Nuclear and New Energy Technology, Tsinghua University, Beijing 100084, China
* Correspondence: lyue@mail.tsinghua.edu.cn

Abstract: A number of canisters need to be lightweight designed to store the spherical fuel elements (SFE) used in high-temperature gas-cooled reactors (HTGR). The main challenge for engineering is pursuing high-accuracy and high-efficiency optimization simultaneously. Accordingly, a hybrid surrogate model-based multi-objective optimization method with the numerical method for the lightweight and safe design of the SFE canister is proposed. To be specific, the drop analysis model of the SFE canister is firstly established where the finite element method—discrete element method (FEM–DEM) coupled method is integrated to simulate the interaction force between the SFE and canister. Through simulation, the design variables, optimization objectives, and constraints are identified. Then the hybrid radial basis function—response surface method (RBF–RSM) surrogate method is carried out to approximate and simplify the accurate numerical model. A non-dominated sorting genetic algorithm (NSGA-II) is used for resolving this multi-objective model. Optimal design is validated using comprehensive comparison, and the reduction of weight and maximum strain can be up to 2.46% and 44.65%, respectively. High-accuracy simulation with high-efficiency optimization is successfully demonstrated to perform the lightweight design on nuclear facilities.

Keywords: SFE canister; lightweight design; surrogate model; hybrid RBF–RSM model

Citation: Hao, Y.; Wang, J.; Lin, M.; Gong, M.; Zhang, W.; Wu, B.; Ma, T.; Wang, H.; Liu, B.; Li, Y. Hybrid Surrogate Model-Based Multi-Objective Lightweight Optimization of Spherical Fuel Element Canister. *Energies* **2023**, *16*, 3587. https://doi.org/10.3390/en16083587

Academic Editors: Dan Gabriel Cacuci, Andrew Buchan, Michael M.R. Williams and Ruixian Fang

Received: 29 March 2023
Revised: 15 April 2023
Accepted: 18 April 2023
Published: 21 April 2023

1. Introduction

The high-temperature gas-cooled reactor (HTGR) is one of the inherently safe Gen-IV advanced reactors. HTGR uses spherical fuel elements (SFE) with a diameter of about 60 mm [1–3]. A number of canisters need to be manufactured to contain the SFEs in the plant. On the one hand, the canisters are required to be designed safe enough to ensure containment for the SFEs under accidental conditions, while on the other hand, the attention on reducing cost and saving resources has been drawn in the whole commercial project [4–6]. Therefore, balancing safety performance and lightweight design has been an urgent task for engineers and manufacturers.

The free drop event is one of the most likely causes, leading to serious damage to the canister. The failure criterion of the storage canister is the safe containment of content under impact loading. The importance of the drop test is indisputable, but the expensive and inconvenient actual test has been the main obstacle. Performing hundreds of canister drop events is impossible and unacceptable. Simulation has become a powerful tool to predict dynamic responses through computer-aided design (CAD) and computer-aided engineering (CAE) projects. The accuracy of the finite element (FE) method based on non-linear explicit technology is well confirmed by the comparison between experiments and simulations in several nuclear cask projects [7–9]. The FE method, coupled with the discrete element method, called FEM–DEM, has been further developed [10] and verified [11] by Lin to simulate the interaction between the SFE and canister in a pebble-bed reactor. His valuable work improves the numerical technology in the field of SFE. Such a method could

consider the force and displacement of each SFE. In the previous study in our lab, the verified FEM–DEM method was employed to predict the safety performance according to the analysis of the HTR-PM600 fresh fuel storage canister [12], and the deformation and displacement of SFEs and containment could be precisely obtained.

The FE-analysis-based optimization has accelerated the process of design. The limitation factor for large-scale optimization based on the high-accuracy FEM–DEM is the computational cost, which is inevitable. There are two mainstream optimization methods. The first is the direct search method. It is often used for one-dimension or linear problems [13]. Combining the classical optimization algorithm and the numerical result, the optimal solutions could be obtained after several iterations. However, for the real-world complex optimization problem, it is hard for FE analysis to explore the whole design space in a short time. Several iterations with a mount of simulations are needed to obtain the optimal solution so that a high computational cost has been observed. At the same time, the unexpected numerical noise sometimes has a negative effect on the processing of direct optimization. The second method is the so-called surrogate model-based optimization. The main idea is introduced as follows: (1) conduct the design of the experiment to generate the sampling points, (2) obtain the responses of the sampling points using the FE method, and (3) construct the surrogate model. The surrogate model has demonstrated the dramatic merits of enhancing computational efficiency and reducing numerical noise. The rapid development of the surrogate model could bring the possibility for high-efficiency optimization based on high-accuracy simulation.

Studies of optimization on the nuclear cask could benefit this work. Generally, their optimization aims to reduce stress or acceleration. Kim optimizes the cushion in the storage wells by changing the thickness of the steel, the density of the foam, and the section of the structure to reduce the Tresca stress of the canister and basket [14]. Hao performs the FE analysis of the impact limiters in spent nuclear fuel casks [15]. Several parameters involving the diameter, height of the impact limiters, and density of foam are chosen as the design variables to minimize the acceleration through the response surface method (RSM). There is a growing body of literature that recognizes the trend of multi-objective optimization. Sharma studies the optimization for a cask that up to a 4.6% reduction in weight and an 8.6% reduction in stress can be observed [16]. The optimization algorithm is a complex search method. Hao performs multi-objective optimization for container transport under multiple impact loading conditions [17]. The optimization of many objectives is well performed to realize a 15.7% improvement in lightweight.

This paper proposes a high-efficiency multi-objective optimization method with a high-accuracy method for the SFE canister. The FEM–DEM method is first used to simulate the interaction between the SFE and the canister, and then the drop model is established. The multi-objective optimization based on the above model on the lightweight and safety performance is established using the hybrid radial basis function—response surface method (RBF–RSM) surrogate model and NSGA-II algorithm. The performance of optimal design has been verified by numerical simulation. The remainder of the paper is structured as follows: Section 2 introduces the proposed optimization procedure, principle, and theory of the FEM–DEM method, surrogate model, and non-dominated sorting genetic algorithm (NSGA-II). Section 3 shows the SFE canister model, boundary conditions, and the initial analysis. Section 4 performs the multi-objective optimization on safety performance and lightweight for the canister. Section 5 discusses and validates the optimal design, while the conclusion is summarized in Section 6.

2. The Optimization Procedure

2.1. Description of the Problem

In this study, the challenge of the high-accuracy and high-efficiency lightweight method for SFE canister is overcome based on integrating the FEM–DEM coupled method, the hybrid surrogate model, and the NASGA-II algorithm. Firstly, the design variables, optimization objectives, and constraints are selected through the FEM–DEM-based simula-

tion result. Then, the Latin hypercube sampling method is adopted to generate uniform points in the design space. After that, the responses of each point are calculated and abstracted through numerical simulation. On this basis, the hybrid RBF–RSM surrogate method is constructed and verified to establish the relationship between the inputs and outputs of the simulation model. The NSGA-II is chosen as the solver for the multi-objective problem to create a set of solutions named the Pareto front. Finally, the optimal solution is validated based on comparing it with the initial solution. The entire process of the proposed optimization method is shown in Figure 1.

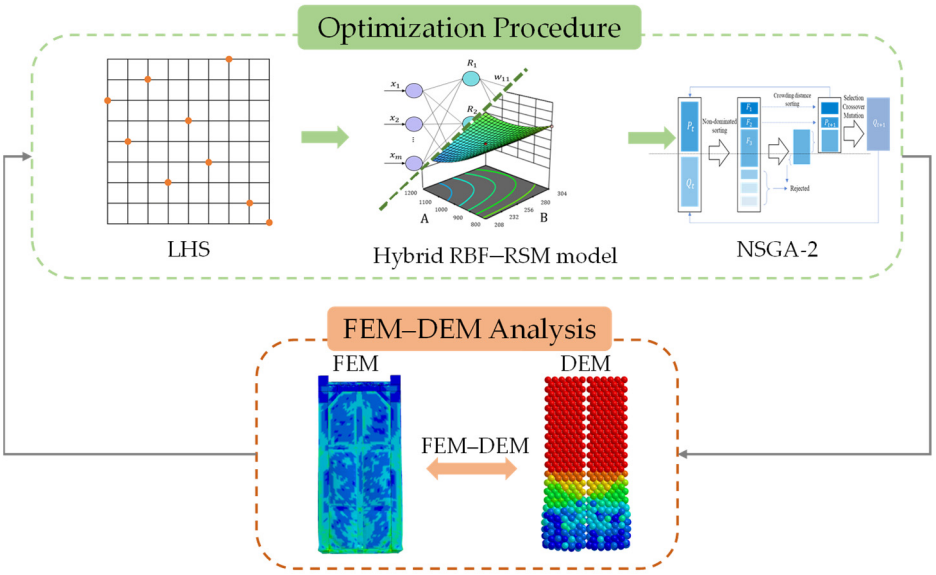

Figure 1. Optimization procedure for SFE canister.

2.2. FEM–DEM Method

The discrete element method (DEM) is first introduced to calculate the contact force between SFEs. The soft sphere model was proposed by Cundall [18] in 1979 and has been widely used in many fields. During the process of contact, an overlap between particles is used to present the deformation at contacting surface. In this model, the normal force adopts the combination of a spring force and a damping force, while the tangential force adopts the combination of three terms: a spring force, a damping force, and a slide force. For the three-dimension SFE considered in this study, the normal force $\boldsymbol{F}_{nij}$ and tangential force $\boldsymbol{F}_{tij}$ could be calculated as follows:

$$\boldsymbol{F}_{nij} = \left(-k_n a^{3/2} - \eta_n \boldsymbol{G}\boldsymbol{n}_{ij}\right)\boldsymbol{n}_{ij} \tag{1}$$

$$\boldsymbol{F}_{tij} = -k_t \boldsymbol{\delta} - \eta_t \boldsymbol{G}_{ct} \tag{2}$$

where a is the overlap in the normal direction, $\boldsymbol{\delta}$ is the tangential displacement, $\boldsymbol{n}_{ij}$ is the vector between the center of two particles, $\boldsymbol{G}$ is the relative velocity, $\boldsymbol{G}_{ct}$ is the sliding velocity; η_n and η_t are the normal and tangential damping coefficient, respectively; k_n and k_t are the normal and tangential stiffness coefficient, respectively.

The interaction force between the SFE and the canister is carried out by referring to the FEM–DEM coupled model [10]. Figure 2 summarizes the FEM–DEM procedure. First, the penetration between the SFE and the canister is detected according to the distance. Then the corresponding contact force and friction force could be obtained based on the penalty method. After that, the displacement of the SFE is obtained with Newton's second law.

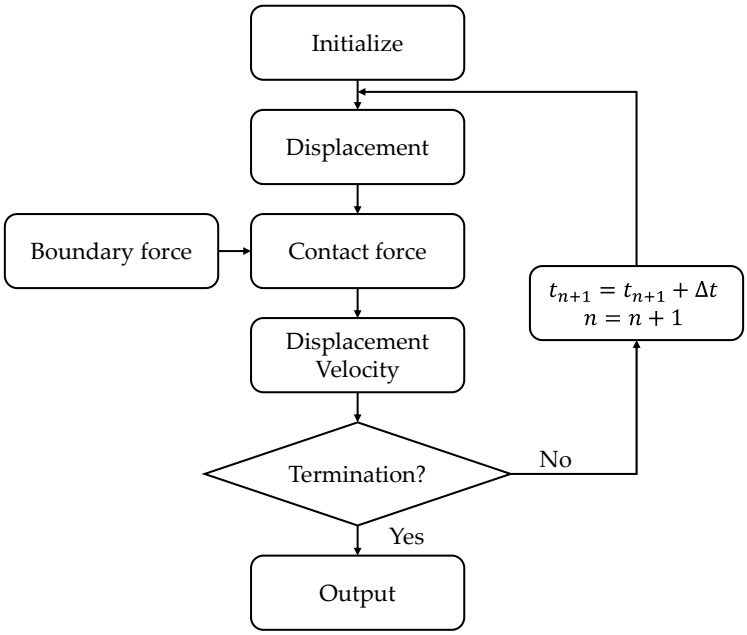

Figure 2. The procedure of FEM–DEM method.

2.3. Surrogate Model

Many optimization problems need a number of simulations or experiments to investigate the responses of the design variables. For a real-world problem, a single simulation could take several hours or even days. For example, a single drop simulation for 100 ms takes approximately 10 h using one 2.1 GHz core of an Intel Xeon CPU. The conventional direct search method has the shortcoming of low efficiency and high cost. To address it, the surrogate model is proposed based on the simplification and approximation of the high-order complex model. There are two main surrogate models considered in this paper, RBF and RSM (Figure 3).

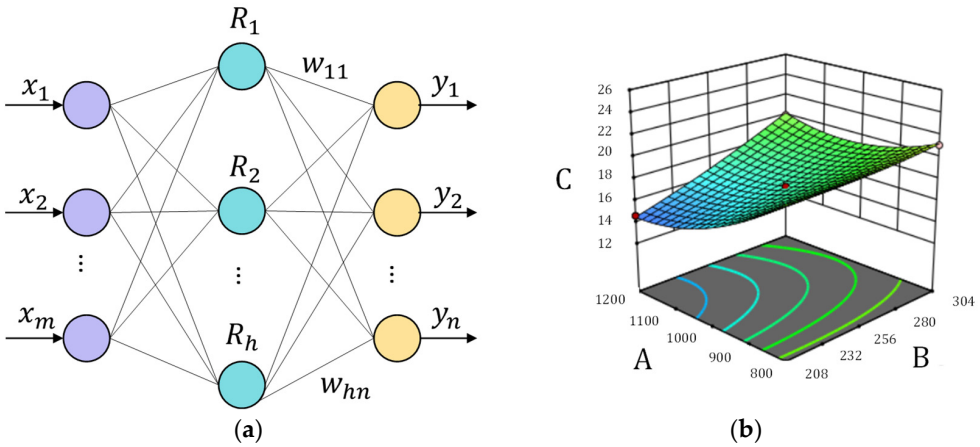

Figure 3. The illustration of (**a**) RBF (**b**) RSM.

RSM (response surface method) employs the polynomial model to explore the relationship between the design and responses, which has the basic formula as follows:

$$f(x) = \beta_0 + \sum \beta_i x_i + \sum \beta_{ij} x_i x_j + \ldots \quad (3)$$

where $f(x)$ is the predicted value, x_i and x_j are the design variables, and β_0, β_i and β_{ij} are the model parameters. It can be seen that the RSM could be more precise if a high-order model is used. However, the increased fitting parameters, which need more simulation

runs, will significantly affect the system's robustness. In fact, the linear model or second-order model is often applied. The polynomial approximations in this study have a linear order with the interaction. The model parameters could be obtained based on the least squares method.

RBF, the so-called radial basis function neural network, is reported as the best neural network-based surrogate model. It has demonstrated the advantages of high efficiency and precision for many non-linear problems. The RBF uses the radial basis function as its activation function. RBF consists of three layers, including an input layer, a single hidden layer, and an output layer. The input layer is linear and transparent and passes a value to the neuron in the hidden layer. The hidden layer is non-linear and contains a variable number of neurons. Each neuron has a radial basis function based on a center point. The output layer performs a linear combination of the results from the hidden layer. The weights between the hidden layer and the output layer are obtained based on Moore–Penrose generalized pseudo-inverse [19]. If the Gaussian function is used as radial basis function ϕ, the output of the RBF φ can be written as follows [20]:

$$\phi(\|x - c_i\|) = e^{-\|x-c_i\|^2/(2\sigma_i{}^2)} \tag{4}$$

$$\varphi = \sum_{i=1}^{h} \lambda_i \phi(\|x - c_i\|) \tag{5}$$

where $\|x - c_i\|$ is the Euclidean distance; c_i and σ_i are the center vector and width of the neuron i in the hidden layer, respectively; h is the number of neurons in the hidden layer. λ_i is the weight between the hidden layer and the output layer. Equation (5) presents the relationship between the neural network input x and output φ. Equation (4) presents the Gaussian function. The search for optimum values of centers, width parameters, and network weights is the basis of the RBF network training process [21]. The data required for the training of the networks are obtained from the numerical simulation and the design of experiment (DOE) results. To be specific, the non-linear mapping relationship between the input parameters (thickness parameters) derived from DOE results and the output parameters (mass, plastic strain, and radial expansion) obtained from numerical simulation is used to train the RBF neural network.

In this paper, the hybrid surrogate method is investigated to approximate the numerical result. In detail, the RBF and RSM methods are both used to construct the relationship between the design variables and structural response. Then the accuracy of the surrogate model for each response is evaluated and compared. After that, the different surrogate technology is selected for a different response to construct the best surrogate model for further optimization.

2.4. NSGA-II Algorithm

An optimization problem often involves two and more conflicting objectives, and a trade-off between these objectives needs to be taken. Differing from the optimization on single objective, there is a set of solutions (i.e., Pareto front) for multi-objective optimization. All of them are equally good. NSGA-II is a powerful multi-objective optimization algorithm with the elitist principle proposed by Deb [22]. It has been widely used in many fields of science and technology. In the procedure of the NSGA-II (Figure 4), the initial parent population P_t is generated randomly, and the offspring population Q_t is created based on the mutation and crossover. Then the non-dominated sorting is performed for the combination of P_t and Q_t to classify them in an ascending order (F_1, F_2, F_3). The best Pareto fronts such as F_1, F_2 are first chosen to transfer to a new parent population P_{t+1}. For fronts such as F_3, crowding distance is calculated to select the extra number of individuals with more distance to fill with the remainder of the population P_{t+1}. Half of the combination of P_t and Q_t is deleted. The new offspring population Q_{t+1} is generated based on the mutation and crossover. The Pareto front could be identified after the given generations.

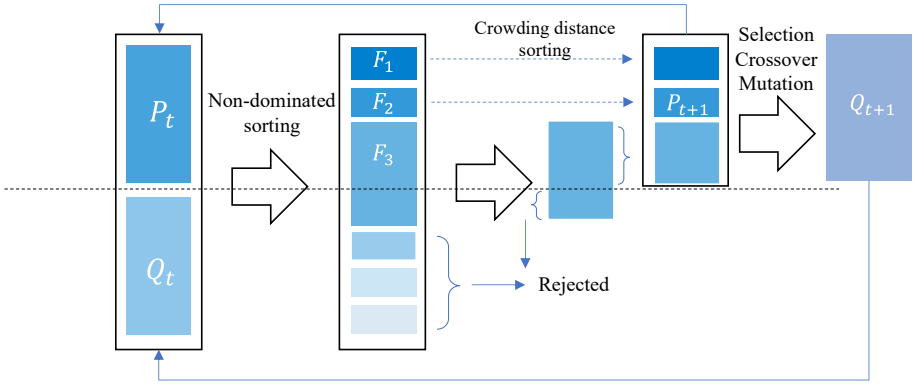

Figure 4. The NSGA-II procedure.

3. SFE Canister Model

3.1. Canister Model

Figure 5 shows the three-dimension model of the SFE canister for containing SFEs and graphite spheres. The cubical shape is designed to save storage space. The size is about $800 \times 800 \times 1800$ mm^3. The canister is a thin-wall structure to realize the lightweight design, including the body, top cover, top flange, frame, and barrier. The top cover is connected to the top flange through 28 × M20 bolts. The topology and shape of the canister are fixed. The optimal combination of the thickness of the main components will be investigated in the next section.

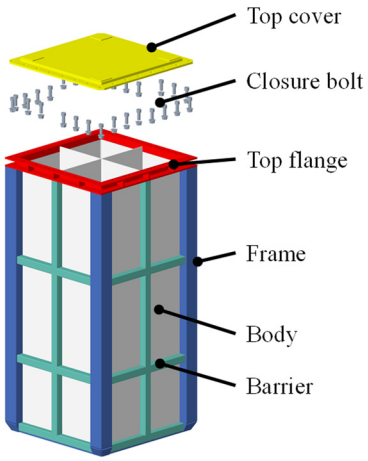

Figure 5. The three-dimension model of the SFE canister.

Figure 6 presents the FE model of canister, which is submitted to the LS-DYNA solver. The Belytschko–Tsay shell elements are adopted to simulate the behavior of thin-wall components because the size of thickness is far less than that of other directions. The thickness of the shell elements is given based on actual data. The integrated point through the thickness is set as 5. The closure bolt with pre-load force is modeled based on the beam element to reflect the tensile and shear stress. The relative sliding and friction between the top cover and the top flange are considered based on the contact algorithm. To improve computational precision, the FE model mainly adopts quadrilateral elements rather than triangular elements. Moreover, element refinement is considered for the area with possible large deformation. The size of the element is set as 20 mm. Based on the above strategies, the FE model has 76,635 elements and 80,581 nodes, where more than 95% of elements are quadrilateral.

The canister is fully manufactured using stainless steel 304. According to the ASME material manual [23], the yield stress and tensile stress are 205 and 520 MPa, respectively. To well simulate the behavior of the material, the piecewise linear plasticity models with

failure are used. The failure criterion is that once the effective plastic strain in one element reaches 40% or the effective stress reaches 520 MPa, the element will be deleted.

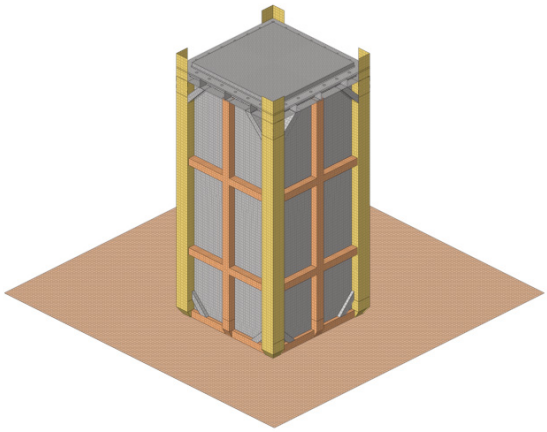

Figure 6. The FE model of the SFE canister.

3.2. SFE Model

For the SFE stored in the canister, the diameter is 60 mm. The material properties are obtained referring to the previous literature [11] as the density of 1.95 g/cm^3, the elastic modulus of 9.8 GPa, and the Poisson ratio of 0.12.

The SFEs employ regular stacking based on the body-centered cubic method to reduce the volume of the pebble bed as much as possible. To be specific, 4800 SFEs are equally loaded into four zones. Each zone has 40 layers, while each layer has 6 × 5 SFEs. Figure 7 shows the SFEs stacking in one zone. The soft-sphere-model-based DEM method is used. The DEM parameters are referred to in the previous literature [12]. The interaction force between the canister and SFE is difficult for the conventional FE method to calculate. The FEM–DEM coupled method is used here. The sliding friction coefficient between the SFE and the canister is 0.2, and the rolling friction coefficient is 0.005.

Figure 7. The illustration of pebble bed.

3.3. The Simulation of Drop Process

The possible accident of the SFE canister is to suffer from a free drop due to the failure of the lifting device. The canister has a maximum height of 15 m from the ground, which is selected as the initial condition in the analysis. To save computational runtime, the distance between the canister and the ground is moved to 0.1 m instead of 15 m with an additional initial velocity of 17.1 m/s, as follows:

$$v = \sqrt{2 \times 9.81 \times (15 - 0.1)} = 17.1 \text{ m/s} \quad (6)$$

During the process of lifting, the canister mainly keeps in a vertical orientation, so it is assumed that the drop test mainly includes a vertical impact which is chosen as the scenario in the following optimization procedure. When the canister contacts the ground, both the canister and the ground may have the deformation to absorb the energy. To conservatively validate the safety performance of the canister under impact loading, the unyielding ground is chosen to increase the damage to the canister as much as possible.

The contact between the canister and ground is considered by activating the keyword in LS-DYNA *CONTACT_AUTOMATIC_SURFACE_TO_SURFACE. Meanwhile, the self-contact of each component is carried out using the keyword *CONTACT_AUTOMATIC_SINGLE_SURFACE. The well-performed contact algorithm could avoid unacceptable penetration and negative sliding energy in the process of simulation.

3.4. Initial Analysis

The LS-DYNA code is used to solve the FE model under impact loading. Three important indicators are abstracted from the simulation result as below:

1. The weight of the SFE canister is 569 kg, which is expected to be designed as light as possible.
2. The effective plastic strain is selected as the safety indicator to describe the deformation of the containment boundary of SFE, with a value of 23.76%.

Figure 8 presents the radial expansion of the sidewall of the containment boundary. It could be found that node 784485 has an expansion with a value of 35.26 mm, which exceeds the limitation of 35 mm.

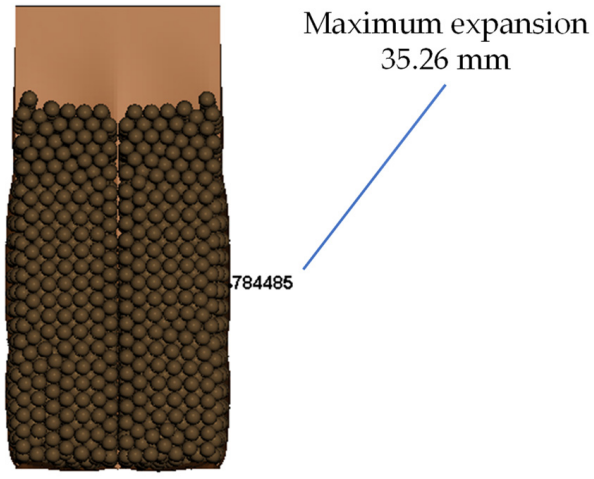

Figure 8. Radial expansion of containment boundary.

Therefore, the optimization objective and constraint could be identified for the further lightweight design. Note that the topology and shape of the thin-wall canister are fixed; thus, the thickness of the main component is chosen as the design variable.

4. Multi-Objective Optimization Problem

4.1. Design Variables and Objective

The aim of optimization for SFE canisters is to improve the performance of lightweight and safety simultaneously. The effective plastic strain of containment boundary (*EPS*) and the weight of the SFE canister (*M*) are selected as the conflicting objective functions. The maximum radial expansion of the canister *(EX)* is chosen as the constraint.

For the canister optimization problems, the thickness parameters of the main components are identified as the design variables. As illustrated in Figure 9, they are the thickness of the canister sidewall (t_1), frame (t_2), and barrier (t_3). Table 1 presents the initial value and range of design variables. The upper and lower limits are determined by engineering experience.

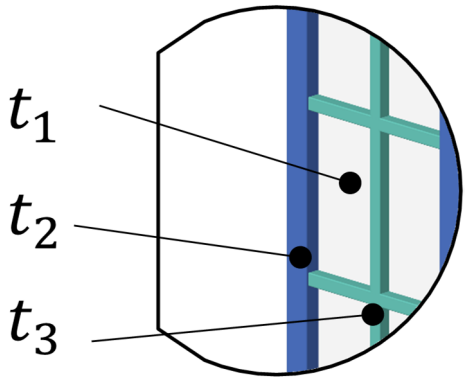

Figure 9. Design variables of SFE canister.

Table 1. Initial value and range of design variables.

Design Variables	Initial Value	Lower Bound	Upper Bound
t_1 (mm)	3	2	6
t_2 (mm)	4	2	6
t_3 (mm)	3	2	6

Once the design variables and the optimization objectives are identified, the multi-objective optimization model could be summarized as follows:

$$\begin{cases} \text{find } \boldsymbol{t} = (t_1, t_2, t_3) \\ \min f(\boldsymbol{t}) = \{f_M(\boldsymbol{t}),\ f_{EPS}(\boldsymbol{t})\} \\ \text{s.t.} f_{EX}(\boldsymbol{t}) \leq 35 \text{ mm} \\ \boldsymbol{t}^L \leq \boldsymbol{t} \leq \boldsymbol{t}^U \end{cases} \tag{7}$$

where $f_M(\boldsymbol{t})$ represents the mass of the SFE canister, $f_{eps}(\boldsymbol{t})$ denotes the effective plastic strain of the boundary containment of the canister; $f_R(\boldsymbol{t})$ stands for the maximum radial expansion of the sidewall; $\boldsymbol{t} = (t_1, t_2, t_3)$ represents the three thickness parameters of the canister sidewall, frame, and barrier; $\boldsymbol{t}^L$ and $\boldsymbol{t}^U$ denote the lower and upper limits of thickness parameters, respectively.

4.2. Surrogate Model Based on LHS

The Latin hypercube sampling (LHS) method is adopted to generate the sampling points as inputs to the surrogate model. To balance the precision and efficiency, 50 points are created based on the LHS method. It can be seen from Figure 10 that the uniform and random distribution of the design variable t_1 demonstrates effective and reliable sampling. The responses (optimization objective and constraint) of each design under impact loading are analyzed using the FE code LS-DYNA, which is summarized in Table 2.

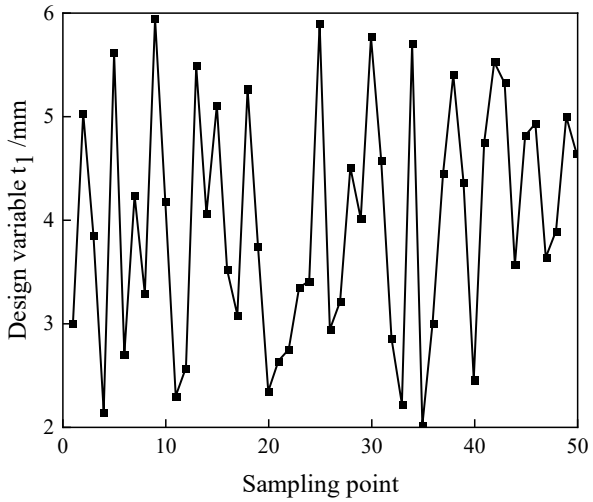

Figure 10. Sampling point of design variable t_1.

Table 2. The response of each design.

No.	Design Variables			Objective		Constraint
	t_1 (mm)	t_2 (mm)	t_3 (mm)	M (kg)	*EPS*	*EX* (mm)
1	3.00	3.00	3.00	552	0.22	38.20
2	5.03	2.00	2.82	618	0.12	34.15
3	3.85	2.41	3.81	600	0.15	33.00
4	2.14	3.42	4.77	568	0.28	41.28
5	5.61	5.50	3.12	711	0.23	26.05
...	...	...	...	...	...	...
49	5.00	4.38	3.98	688	0.19	33.36
50	4.64	2.53	2.04	590	0.14	33.20

The next step is to construct the relationship between the design variable and the optimization objective based on the surrogated model. To select the best surrogate model method, the RSM and RBF are used. For the RSM model, the model with quadratic terms has better performance than a linear model for fitting non-linear data. To evaluate the accuracy of the selected surrogate models, two indicators are chosen, they are the coefficient of determination R^2 and root mean square error (RMSE), which could be calculated as follows:

$$R^2 = \frac{\Sigma_i^P (\hat{y}_i - \overline{y})^2}{\Sigma_i^P (y_i - \overline{y})^2} \tag{8}$$

$$\text{RMSE} = \sqrt{\frac{\Sigma_i^P (y_i - \hat{y}_i)^2}{P}} \tag{9}$$

where, y_i is the actual response, $\overline{y}$ is the average of the actual response, $\hat{y}_i$ is the predicted value from the surrogate model, P is the number of designs. The bigger the coefficient of determination R^2 and the smaller the RMSE, the higher precision the model has. When $R^2 > 0.85$ and RMSE < 0.1, the surrogate model is able to well establish the relationship between the design variables and objectives for further optimization

Table 3 presents the accuracy of the RBF and RSM surrogate models. The R^2 of RBF and RSM for the mass (M) are basically equal to 1 as the RMSE of the two models is smaller than 0.01%. The fitting accuracy is significantly higher than others because the mass is a linear response according to the design variables. The RBF method has a higher value of R^2 and a lower value of RMSE for the effective strain, while the RSM model has a higher value of R^2 and a lower value of RMSE for the radial expansion. Therefore, the hybrid RBF–RSM

method is finally used to generate the surrogate model to approximate the relationship between the design variables, optimization objective, and constraint. Especially the mass and effective response are fitted using the RBF method, as the radial expansion response is fitted using the RSM method. The R^2 in the hybrid surrogate model is more than 0.85, while the RMSE is lower than 0.1. Figure 11 shows the fitting result of the surrogate model. To better understand the fitting accuracy, the comparison between the simulation result and the predicted value is shown in Figure 12. The x-axis denotes the value based on numerical simulation, while the y-axis denotes the predicted value based on the surrogate model. From Figure 12, most of the points are close to the 45-degree line, indicating that the predicted value is approximately equal to the calculated value. Combined with the R^2, RMSE, and the simulation-prediction comparison, it can be summarized that the hybrid approximate surrogate model has great accuracy and reliability, which could be used for predicting the responses well.

Table 3. The accuracy of the surrogate model.

	RBF		RSM	
	R^2	RSME	R^2	RSME
Mass	1	0.00233%	1	0.00218%
Effective strain	0.985	2.33%	0.897	7.72%
Radial expansion	0.818	4.42%	0.874	4.1%

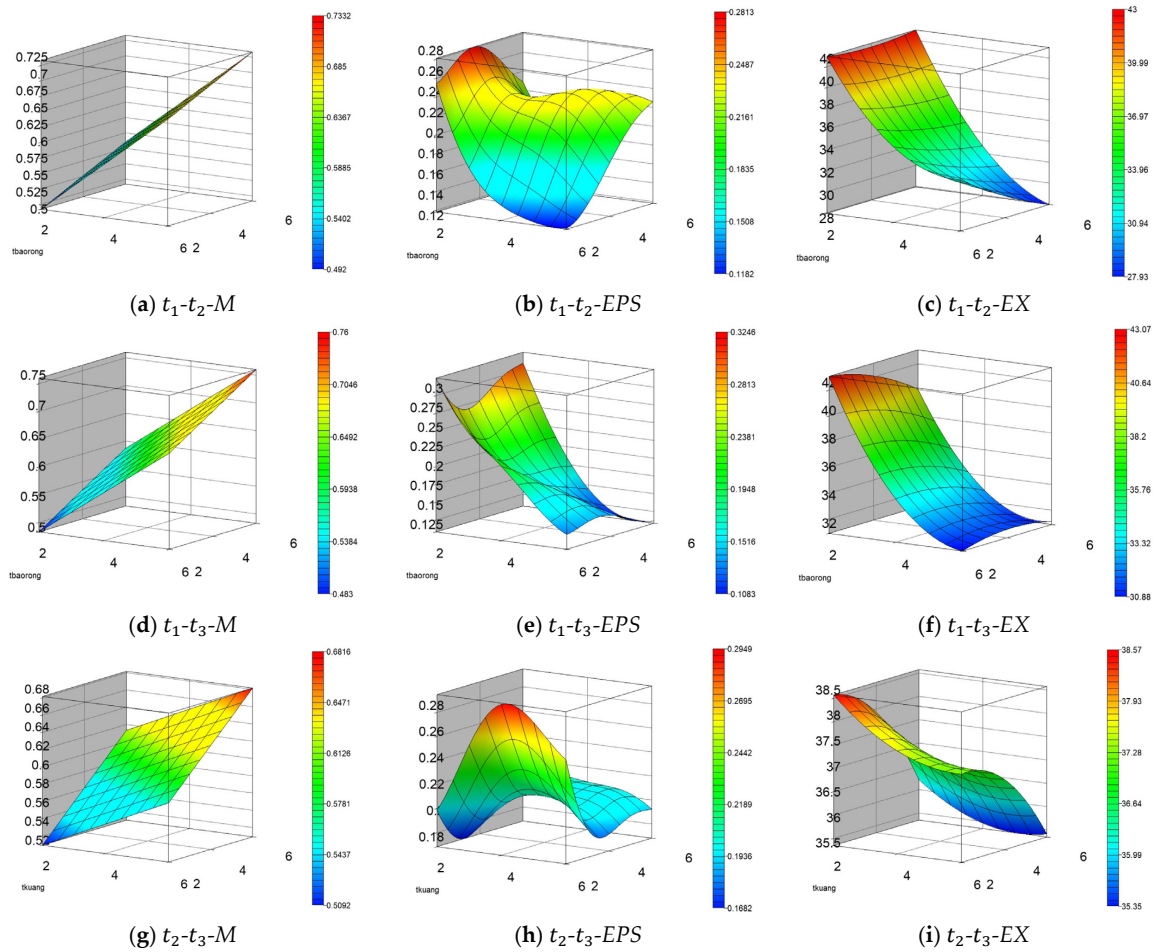

(**a**) t_1-t_2-M (**b**) t_1-t_2-EPS (**c**) t_1-t_2-EX

(**d**) t_1-t_3-M (**e**) t_1-t_3-EPS (**f**) t_1-t_3-EX

(**g**) t_2-t_3-M (**h**) t_2-t_3-EPS (**i**) t_2-t_3-EX

Figure 11. The result of surrogate model.

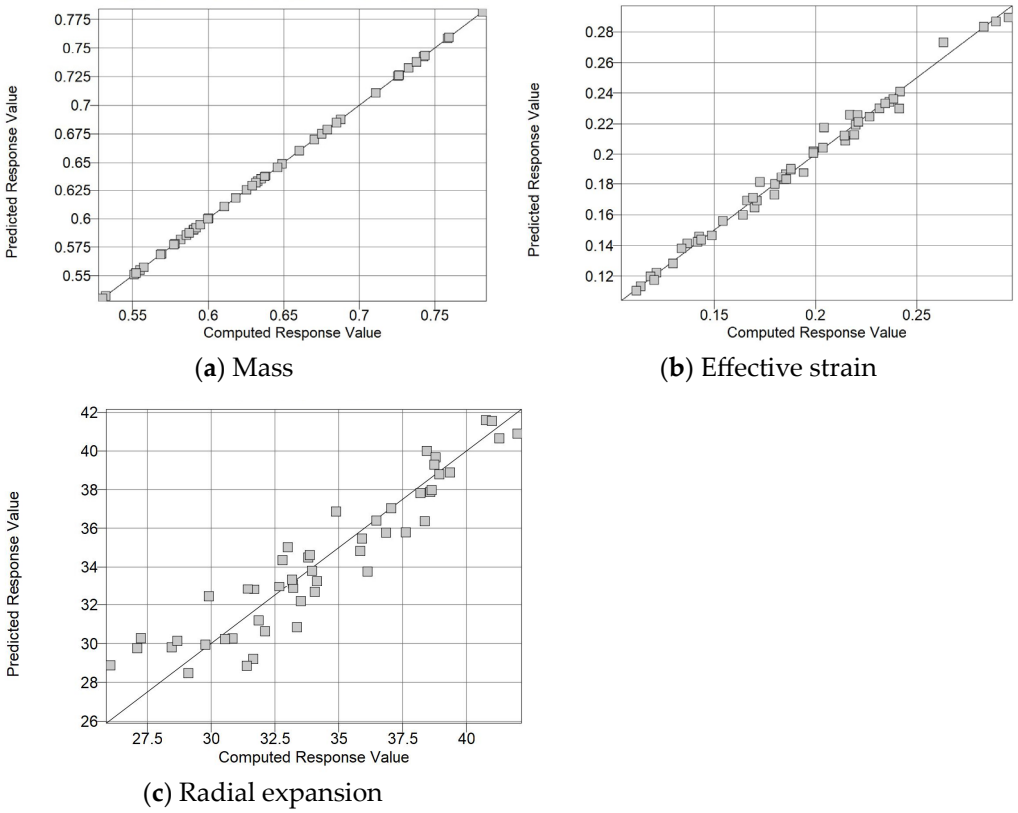

(**a**) Mass (**b**) Effective strain

(**c**) Radial expansion

Figure 12. Comparison between the simulation result and the predicted value.

5. Result and Discussion

The optimization of minimizing the mass and effective strain with the constraints of the maximum radial expansion is, in fact, a multi-objective problem. To address it, the multi-objective optimization procedure NSGA-II is used as the solver. The detailed parameters of the algorithm are summarized in Table 4. After 25,000 runs, the optimization could be completed because of the high efficiency of NSGA-II.

Table 4. NSGA-II parameters.

Parameter	Value
Population size	100
Number of generations	250
Crossover distribution	10
Crossover probability	1
Mutation distribution	100
Mutation probability	0.33

On the basis of the NSGA-II, the Pareto front could be obtained, as shown in Figure 13. The *x*-axis in the figure presents the mass, while the *y*-axis presents the effective strain of the containment boundary of SFEs under impact loading. The value of maximum radial expansion is illustrated using a color gradient with a range from 32.54 to 34.98 mm. It could be found that the radial expansions of all designs are lower than 35 mm, indicating that the Pareto solutions could satisfy the optimization model in Equation (1). The Pareto front denotes a set of effective solutions which are equally important. The so-called non-dominated solution indicates that one solution could not dominate others when considering the whole objective simultaneously. Note that the maximum effective strain (0.135) is far less than the limit (0.4), which is totally acceptable. Thus, the design with the maximum stain

and minimum mass is selected as the optimal design ($t_1 = 4.06$ mm, $t_2 = 2$ mm, $t_3 = 2$ mm).

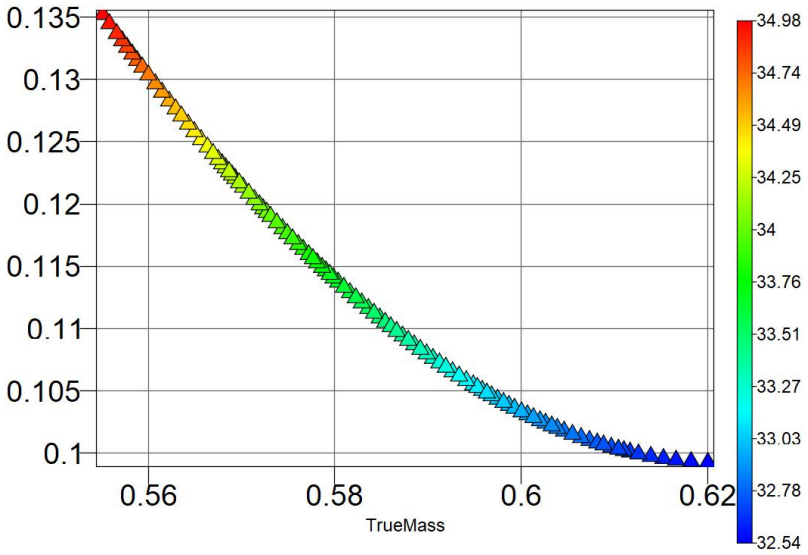

Figure 13. Pareto front.

Table 5 shows the relative error between the predicted value from the surrogate model and the calculated value from the numerical simulation. It could be seen that the relative errors of the responses are less than 5%, which indicates that the surrogate model we chose is reliable.

Table 5. The error between the surrogate model and numerical simulation.

Response	Predicted Value	Calculated Value	Relative Error
Mass (kg)	554.8	555	0.04%
Effective strain	13.55%	13.15%	3.04%
Radial expansion (mm)	35.0	34.8	0.57%

To verify the merits of the optimal design, the comparison is carried out using the FE analysis between the initial design and the optimal design, as listed in Table 6. It can be seen that all the indicators have been improved. The canister has a mass reduction of 14 kg and a successful improvement of 2.46%, which is well lightweight designed compared to the initial design. In addition, the effective strain of containment and the radial expansion is finally reduced by 44.65% and 2.3%, respectively. The result shows that the optimal design is within the great performance threshold.

Table 6. Performance comparison.

Response	Initial Design	Optimal Design	Improvement
Mass (kg)	569	555	2.46%
Effective strain	23.76%	13.15%	44.65%
Radial expansion (mm)	35.79	34.97	2.3%

Figure 14 shows the radial expansion curve of the initial design and the optimal design at node 784485. It can be seen that the two curves are overall similar. However, the initial design has a larger peak than the optimal design. It is because the optimal design has more stiffness after the optimization, which decreases the expansion of the side wall of the SFE canister.

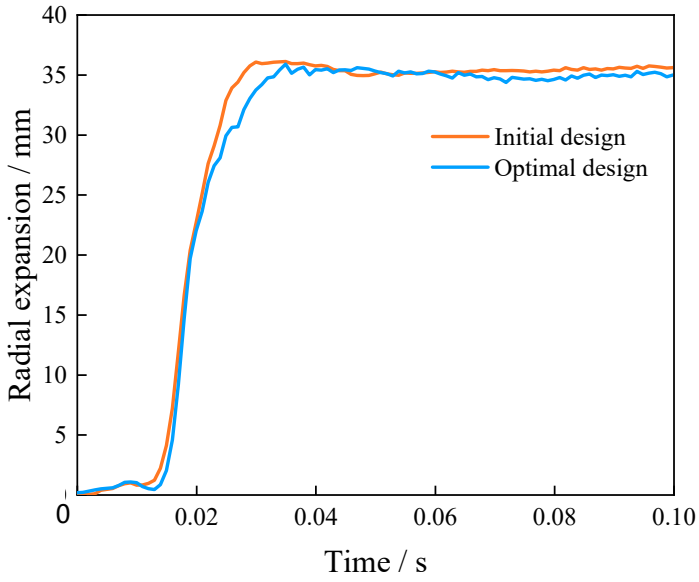

Figure 14. Radial expansion comparison.

Figure 15 shows the maximum interaction force between the pebble bed and the canister from the simulation result. The value and distribution are compared between the initial design and the optimal design. It could be seen that the maximum force is 6.295 and 6.223 kN before and after optimization, which has a reduced ratio of 1.14%. In fact, the decreased interaction force could ensure the integrity of the fuel element.

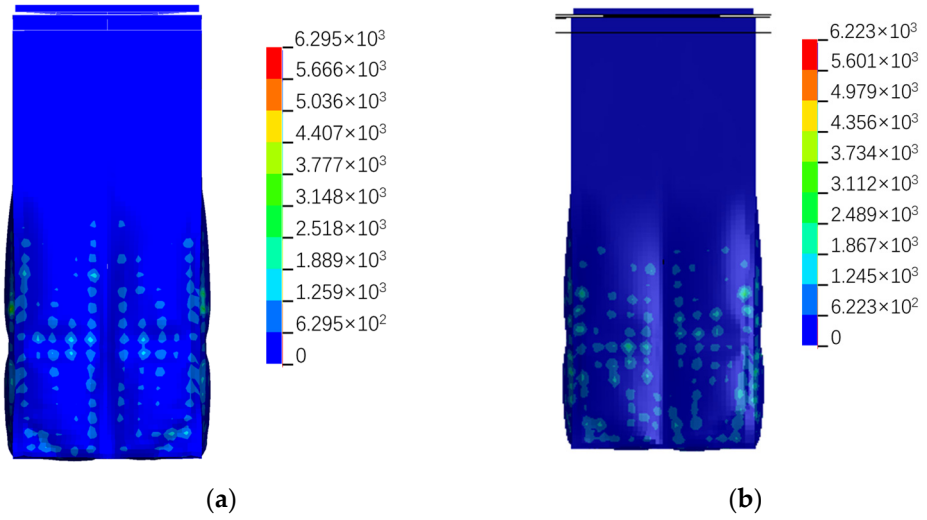

Figure 15. The interaction force (**a**) initial design and (**b**) optimal design.

In summary, the multi-objective optimization could not only reduce the weight of the canister but also improve safety performance.

6. Conclusions

This paper presents an efficiency–accuracy balanced lightweight optimization procedure for the SFE canister, integrating the FEM–DEM coupled method, the Latin hypercube sampling, the RSM-RBF-based hybrid surrogate model, and the NSGA-II algorithm. Based on the study, the following conclusion could be summarized:

1. The deformation and displacement of the canister and SFEs under impact loading could be obtained through the drop analysis model integrating the FEM–DEM method.

2. The hybrid RBF–RSM model has been validated with high accuracy based on R^2, RMSE, and the simulation-prediction comparison. It is believed to approximate precisely the accurate but high-cost simulation model.
3. The calculation result shows that up to 2.45% reduction of mass and 44.65% reduction of the plastic strain could be realized, while the optimal canister can protect SFEs well in the extreme event, indicating the multi-objective lightweight canister is designed successfully.
4. In future investigations, it might be possible to consider shape optimization, topological optimization, and multidisciplinary design optimization for expansion.

Author Contributions: Conceptualization, Y.H., J.W. and Y.L.; methodology, Y.H.; software, Y.H.; validation, M.L. and W.Z.; investigation, M.L., M.G., B.W., T.M., H.W. and B.L.; resources, M.G., B.W., T.M., H.W. and B.L.; data curation, M.L. and M.G.; writing—original draft preparation, Y.H.; writing—review and editing, Y.H., M.L. and W.Z.; visualization, M.L. and M.G.; supervision, Y.L.; project administration, J.W. and Y.L.; funding acquisition, J.W. All authors have read and agreed to the published version of the manuscript.

Funding: This work has been supported by the National S&T Major Project (Grant No. ZX069) provided by the National Energy Bureau of China and the Modular HTGR Super-critical Power Generation Technology collaborative project between CNNC and Tsinghua University (Project No. ZHJTJZYFGWD2020).

Data Availability Statement: Not applicable.

Conflicts of Interest: The authors declare no conflict of interest.

References

1. Kugeler, K.; Zhang, Z. Fuel Elements. In *Modular High-Temperature Gas-Cooled Reactor Power Plant*; Springer: Berlin/Heidelberg, Germany, 2019. [CrossRef]
2. Li, L.; Yuan, H.; Wang, K. Coupling of RMC and CFX for analysis of Pebble Bed-Advanced High Temperature Reactor core. *Nucl. Eng. Des.* **2012**, *250*, 385–391. [CrossRef]
3. Alrwashdeh, M.; Alameri, S.; Alkaabi, A. Preliminary Study of a Prismatic-Core Advanced High-Temperature Reactor Fuel Using Homogenization Double-Heterogeneous Method. *Nucl. Sci. Eng.* **2020**, *194*, 163–167. [CrossRef]
4. El-Samrah, M.; Tawfic, A.; Chidiac, S. Spent nuclear fuel interim dry storage; Design requirements, most common methods, and evolution: A review. *Ann. Nucl. Energy* **2021**, *160*, 108408. [CrossRef]
5. Ali, M.; Tawfic, A.; Abdelgawad, M.; Wagih, M.; Omar, A. Potential uses of different sustainable concrete mixtures in gamma and neutrons shielding purposes. *Prog. Nucl. Energy* **2023**, *157*, 104598. [CrossRef]
6. Ali, M.; Tawfic, A.; Abdelgawad, M.; Mahdy, M.; Omar, A. Gamma and neutrons shielding using innovative fiber reinforced concrete. *Prog. Nucl. Energy* **2022**, *145*, 104133. [CrossRef]
7. Kim, K.-S.; Chung, S.-H.; Kim, J.-S.; Choi, K.-S.; Yun, H.-D. Demonstration of structural performance of IP-2 packages by advanced analytical simulation and full-scale drop test. *Nucl. Eng. Des.* **2010**, *240*, 639–655. [CrossRef]
8. Kim, K.-S.; Kim, J.-S.; Choi, K.-S.; Shin, T.-M.; Yun, H.-D. Dynamic impact characteristics of KN-18 SNF transport cask—Part 1: An advanced numerical simulation and validation technique. *Ann. Nucl. Energy* **2010**, *37*, 546–559. [CrossRef]
9. Wu, T.-Y.; Lee, H.-Y.; Kang, L.-C. Dynamic response analysis of a spent-fuel dry storage cask under vertical drop accident. *Ann. Nucl. Energy* **2012**, *42*, 18–29. [CrossRef]
10. Lin, M.; Li, Y. Analysis of the interactions between spent fuel pebble bed and storage canister under impact loading. *Nucl. Eng. Des.* **2020**, *361*, 110548. [CrossRef]
11. Lin, M.; Wang, J.; Wu, B.; Li, Y. Dynamic analysis of dry storage canister and the spent fuels inside under vertical drop in HTR-PM. *Ann. Nucl. Energy* **2021**, *154*, 108030. [CrossRef]
12. Hao, Y.; Wang, J.; Wang, H.; Liu, B.; Li, Y. Safety performance of HTR-PM600 fresh fuel storage canister under drop impact. *Qinghua Daxue Xuebao/J. Tsinghua Univ.* **2022**, *62*, 1668–1674. [CrossRef]
13. Wang, C. Structure-Material-Performance Integration Lightweight Multi-Objective Collaborative Optimization Design for Front Structure of BIW. Ph.D. Thesis, Jilin University, Changchun, China, 2015.
14. Kim, D.-H.; Seo, K.-S.; Lee, J.-C.; Bang, K.-S.; Cho, C.-H.; Lee, S.J.; Baeg, C.Y. Finite element analyses and verifying tests for a shock-absorbing effect of a pad in a spent fuel storage cask. *Ann. Nucl. Energy* **2007**, *34*, 871–882. [CrossRef]
15. Hao, Y.; Wang, J.; Li, Y.; Wu, B.; Wang, H.; Ma, T. Study on the structural evaluation and optimization of spent nuclear fuel cask. In Proceedings of the International Conference on Nuclear Engineering, Online, 4–6 August 2021.
16. Sharma, K.; Pawaskar, D.N.; Guha, A.; Singh, R.K. Optimization of cask for transport of radioactive material under impact loading. *Nucl. Eng. Des.* **2014**, *273*, 190–201. [CrossRef]

17. Hao, Y.; Li, Y.; Wu, B.; Ma, T.; Wang, H.; Liu, B.; Wang, J. Optimization analysis of HTR-PM600 fresh fuel transport container under multiple impact loading conditions. *Ann. Nucl. Energy* **2022**, *175*, 109216. [CrossRef]
18. Cundall, P.A.; Strack, O.D.L. A discrete numerical model for granular assemblies. *Géotechnique* **1979**, *29*, 47–65. [CrossRef]
19. Alireza. Radial Basis Function Neural Networks (with Parameter Selection Using K-Means). MATLAB Central File Exchange. 2022. Available online: https://www.mathworks.com/matlabcentral/fileexchange/52580-radial-basis-function-neural-networks-with-parameter-selection-using-k-means (accessed on 15 August 2022).
20. Faris, H.; Aljarah, I.; Mirjalili, S. Chapter 28—Evolving Radial Basis Function Networks Using Moth–Flame Optimizer. In *Handbook of Neural Computation*; Samui, P., Sekhar, S., Balas, V.E., Eds.; Academic Press: Cambridge, MA, USA, 2017; pp. 537–550.
21. Zhang, D.; Wang, C.; Wei, Y.; Yang, L. Analysis of motion interference characteristics of underwater vehicles salvo ased on the RBF Neural Network. *Ocean Eng.* **2023**, *277*, 114254. [CrossRef]
22. Deb, K.; Pratap, A.; Agarwal, S.; Meyarivan, T. A fast and elitist multiobjective genetic algorithm: NSGA-II. *IEEE Trans. Evol. Comput.* **2002**, *6*, 182–197. [CrossRef]
23. American Society of Mechanical Engineers. *ASME BPVC Section II Part D Properties (Customary)*; The American Society of Mechanical Engineers: New York, NY, USA, 2015.